JOURNAL OF MATERIALS SCIENCE 28 (1993) 3951–3956

# EPR structural study on hydrothermally aged yttria-doped tetragonal zirconia polycrystals

C. B. AZZONI, A. PALEARI*, F. SCARDINA
*Department of Physics "A. Volta", University of Pavia, via Bassi 6, I-27100 Pavia, Italy*
A. KRAJEWSKI, A. RAVAGLIOLI, F. MESCHKE
*Institute for Technological Research on Ceramics (IRTEC) of CNR, Faenza, Italy*

EPR measurements on yttria-doped tetragonal zirconia polycrystals (Y–TZP) were performed in order to study the modifications of the structure of the material following hydrothermal treatments. By X-ray irradiation of the samples, the structural defects near the oxygen vacancies were magnetically activated by electron trapping. $Y_2O_3$ aggregates were identified by EPR signals of defects of $F^+$ type, coordinated with yttrium ions, and defects such as $Y^{2+}$ ($4d^1$) in four-fold coordination, randomly tetragonally distorted. The analysis of these defect sites, used as local probes, supports the existence of structural modification of the material and the formation of $\alpha$-$Y(OH)_3$ clusters.

## 1. Introduction

Zirconia ($ZrO_2$) is a promising material for a wide number of technological and engineering applications [1]. Apart from its good chemical stability due to the strong Zr–O chemical bond, it exhibits outstanding mechanical properties. High strength and toughness can be achieved by adding some kinds of oxides in a narrow range of composition; the most commonly used are MgO, CaO, $Y_2O_3$ and $CeO_2$. These oxides act to retain the high-temperature phase of zirconia at room temperature at which it is normally in the monoclinic phase. The cations of such added substances randomly substitute the $Zr^{4+}$ cations in their lattice sites and are therefore called lattice stabilizers. Depending on the amount of stabilizer, a tetragonal phase can be retained in a high volume fraction.

Yttria-doped tetragonal zirconia polycrystals (Y-TPZ) is one of the zirconia-based materials with very high strength and toughness. However, attention to the use of this kind of stabilized zirconia is directed at hydrothermal treatments occurring when the environment is constituted by hot steam. In fact, in a humid atmosphere at relatively low temperatures (about 200 °C), an uncontrolled tetragonal-to-monoclinic transformation occurs resulting in microcracking and strength degradation [2, 3]. Several theories have been proposed in order to explain the mechanism involved, in which atomic positions are rearranged, leading to the transformation.

One theory proposes the breaking of the bonds of the oxygen bridge Zr–O–Zr with formation of Zr–OH bonds [4]; more elaborate evolutions of this theory propose multi-step degradation processes, also resulting in the formation of Zr–OH bonds which create stress sites [5, 6]. Another theory involves the production of nanometric $\alpha$-$Y(OH)_3$ which draws yttrium from the grains of zirconia in the tetragonal phase, as experimentally observed [7, 8]. Parts of the volume of the zirconia crystal lattice, which lack stabilizing ions, can therefore easily transform into monoclinic nuclei which grow with further yttrium depletion, until the complete transformation of the whole grain. Microcracks occurring on the surface of the ceramic piece allow the process of transformation to proceed into the bulk.

However, only a few structuristical experiments have been performed to study the atomic rearrangement. The study of the intrinsic defects due to oxygen vacancies or associated with the presence of substitutional cations, is a fundamental step to control the physical–mechanical properties of this material.

A detailed analysis by electron paramagnetic resonance (EPR) has already been carried out on single crystals of yttria-stabilized zirconia. That analysis was focused on identifying the structure of the main paramagnetic defects induced either by chemical reduction or ultraviolet and X-ray irradiation [9]. The EPR centres were found to be sensitive probes, able to provide information on the local nanostructure of the material, thus giving detail of the arrangement of the anionic sublattice [10, 11]. On the other hand, analogous spectroscopic data are not available on sintered samples, in spite of the large number of possible technological applications of this ceramic material.

In this paper we report EPR measurements on ceramic samples of zirconia stabilized by the addition of 3 mol % yttria ($Zr_{0.97}Y_{0.03}O_{1.99}$). The experimental spectrum was resolved into the different components by analysing the dependence on the measuring temperature and the microwave power,

* *Permanent address*: Dipartimento di Fisica, Universita' di Milano, via Celoria 16, I-20133 Milano, Italy.

0022–2461  

and on thermal annealing. Further details of the surface structure of the material were obtained by using the paramagnetic defects induced by X-ray irradiation as local probes. Using these data, an attempt is made to explain the processes leading to brittleness of surgical tools made of this material exposed to short hydrothermal treatments (e.g. sterilization procedures of bistouries by autoclaving).

## 2. Experimental procedure

### 2.1. Composition and production of the samples

A series of bars, with dimensions $20 \times 1 \times 0.5$ mm$^3$ after sintering, were produced. These samples were prepared for this study using the same procedure utilized to produce prototypes of ceramic bistouries in IRTEC-CNR. As starting materials, zirconia powders stabilized with 3 mol % $Y_2O_3$ were used (TSK TZ-3Y, Toyo Soda Mfg. Co. Ltd, Japan). Such prototypes were produced under a project devoted to the development of ceramic materials for use in surgery and are the subject-matter of a thesis for Design and Ceramic Technology Certificate coordinated by the IRTEC-CNR authors of this paper [12].

For the adopted manufacturing process, the green samples were prepared by mixing the utilized powders with a 2 M solution of polyethyleneglycol PeG-300 [$HO(C_2H_4O)_nH$]. The mixture was carefully milled for 20 h with water in a jar-mill with zirconia milling balls. The obtained slurry was freeze-dried and the powders obtained were sieved. The powders were then pressed uniaxially at 6.1 MPa by a double-effect press.

The sintering of the samples was carried out in a programmable laboratory kiln with the adoption of the following thermal cycle: temperature raised to the sintering temperature of 1500 °C by a linear increment of 100 °C h$^{-1}$; hold at the sintering temperature for 1 h; cooled at 300 °C h$^{-1}$.

All the sintered samples were carefully polished with a 0.3 μm diamond paper on their surface to eliminate superficial defects.

### 2.2. EPR measurements

EPR measurements were carried out on the samples using a spectrometer in the X band (about 9.12 GHz) in the temperature range − 135 to 30 °C. A cryostat with a nitrogen flux and a temperature control within 1 °C, were used for this purpose. The modulation field was kept down to suitably low values to avoid signal distortions. Different values of the incident radiation power were used, 1–10 mW, to keep saturation phenomena under control. The EPR centres concentration was estimated with respect to a standard, by measuring the weight and volume of the samples, and having particular care to the reproducibility of the positioning of the samples in the resonant cavity. The interpretation of the EPR spectra was verified by numerical methods of simulation of resonance signals of polycrystalline materials (such as powders and glasses), i.e. of signals originating from paramagnetic centres randomly oriented and characterized by a $g$ tensor with a gaussian distribution of principal values.

### 2.3. X-ray diffraction analysis

Samples (prepared in the same way as those for EPR measurements) were analysed by X-ray diffractometry. A Rigaku powder diffractometer was used to test the phase composition directly on the surface of the samples.

### 2.4. Treatments

Some ceramic samples were treated before any measurement in an autoclave with a hot water vapour atmosphere. This treatment should simulate the operative conditions of contact with steam in turbines and in sterilization procedures adopted in surgery, which are known to cause transformations within the microstructure of the material.

The treatment involved a run in the autoclave at medium pressure (500 ± 20 kPa) at 160 °C. These values were reached gradually over 1 h and then they were held steady for 1 h. At the end, the pressure was suddenly removed and the samples cooled within the autoclave in 0.5 h.

Some samples, treated both in an autoclave and untreated, were heated at 850 °C in air for 2 h followed by natural cooling to room temperature, in order to observe the stability of the centres and the effects of the hydroxylation of possible hydroxyl groups induced by the autoclave treatments. Other samples, treated and untreated in the autoclave, were exposed to X-ray irradiation at room temperature, using a beam of about 15 keV from a tungsten target: because structural defects may be present in diamagnetic form (undetectable by EPR), X-ray irradiations were performed in order to activate such defect sites by electronic trapping. The X-ray irradiation treatments do not modify the atomic arrangement of the structure, and allow a selective activation of the material by choosing the suitable photon energy with the desired attenuation depth.

Isochronal annealings were carried out to discriminate EPR signals characterized by different thermal stability by leaving the samples for 5 min in a thermostated furnace at a prefixed temperature, at normal pressure and in air.

## 3. Results

### 3.1. Virgin samples

Although the EPR spectra obtained were highly complex, three types of signal could be identified (Fig. 1):

(a) a narrow, intense signal at low magnetic fields (about 150 mT) having a $g$ value around 4.3 (see insert in the Fig. 1a);

(b) a weak and unstructured signal with $g \simeq 2$;

(c) an asymmetric signal composed of two structures with $g = 1.97$ and 1.96.

The shape and position of signal (a) are typical of ions with spin $S = 5/2$ and with orbital angular moment $L = 0$ such as $Fe^{3+}$ [13]. The concentration of

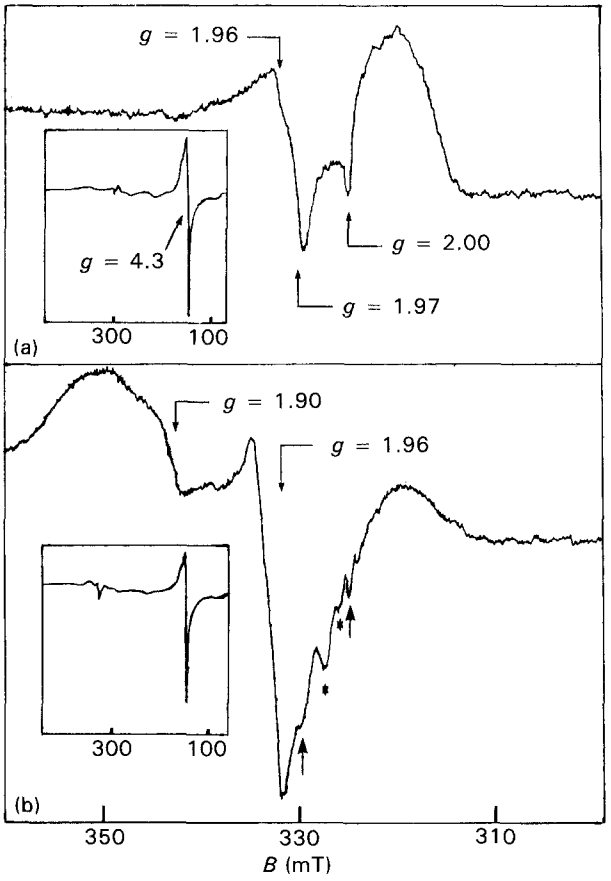


*Figure 1* EPR spectra of a sintered sample of $Zr_{0.97}Y_{0.03}O_{1.99}$ at −135 °C : (a) before and (b) after X-ray irradiation.

this ion is estimated to be about $10^{17}$ cm$^{-3}$ for all the samples.

Signal (b) is very weak and the defects responsible for this resonance should have a concentration of about $5 \times 10^{15}$ cm$^{-3}$.

Signal (c) shows a change in its shape on increasing the temperature from − 135 °C to 30 °C. This change depends on the structure at $g = 1.97$ alone. This suggests that signal (c) is composed of two different signals. The evaluated density of the correspondent paramagnetic centres is about $10^{15}$ cm$^{-3}$.

The corresponding X-ray diffraction spectra show the presence of tetragonal phase, with some traces of cubic phase.

## 3.2. Effects of autoclave treatment

The EPR spectrum of the samples treated in the autoclave differs from that of the virgin samples only for signal (c) which is more intense. It is noteworthy that segmentation of the samples into pieces with different surface/volume ratios shows that signal (a) has an intensity that is proportional to volume, while signals (b) and (c) have amplitudes which do not depend on the volume, but rather on the surface of the sample.

All the identified signals are very stable and no decrease in their magnitude was observed, even after a prolonged heating of 2 h at 850 °C.

The corresponding X-ray diffraction spectra show a predominance of tetragonal phase, but with the appearance of a small amount of monoclinic phase and some weak but significant peaks attributable to $Y_2O_3$.

## 3.3. Irradiated samples

The spectrum of an irradiated sample is shown in Fig. 1b. In addition to some structures (arrowed) attributable to signals already present in the unirradiated samples and unaffected by the irradiation, some other structures can be identified:

(A) a portion of a signal about 6 mT wide, structured, at fields higher than 340 mT, with $g = 1.90$;

(B) an asymmetrical narrower signal (3 mT wide) at $g = 1.96$, which overlaps signal (c) observed in the unirradiated samples;

(C) other weaker signals overlapping signal (B) (asterisks in Fig. 1b).

The spectrum induced by the irradiation in the sample treated in the autoclave, although preserving the same characteristics, shows a weaker intensity of signal (A) with respect to the untreated samples.

## 3.4. Thermal annealing of irradiated samples

Isochronal annealing at increasing temperatures has allowed identification of the spectra obtained from the irradiated samples, because the different spectral components show different thermal stabilities. The spectrum of a sample, only just irradiated, is shown in Fig. 2 together with those of the same sample

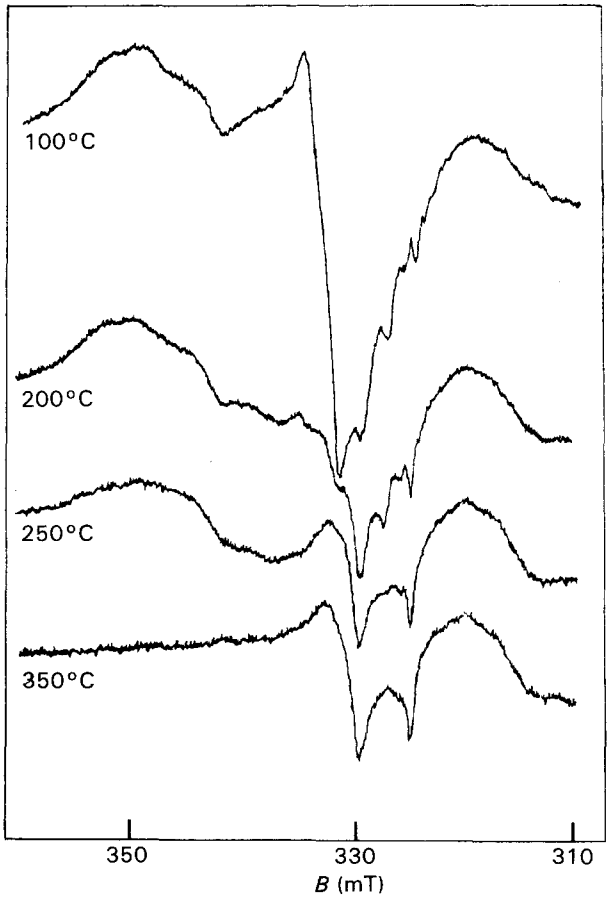


*Figure 2* EPR spectra at − 135 °C following pulsed annealing of 5 min at the indicated temperatures.

after heating for 5 min at different temperatures. At 250 °C, signal (B) is practically absent, whilst signal (A) (whose structured shape is easier to investigate because it does not overlap with other signals) is shown to have a slightly reduced intensity.

## 4. Discussion

The analysed spectra show the complexity typical of spectra of sinterized materials, with powder signals, often overlapping with extrinsic signals of paramagnetic impurities not always identifiable by the EPR technique alone.

A detailed study of the signals cannot always be carried out on sintered materials, unlike for single crystals on which the analysis of the spectrum may be performed as a function of the orientation of the crystallographic axes with respect to the direction of the magnetic field. However, a study of the dependence of the signals upon the different treatments described here has allowed an analysis, qualitative and quantitative, of the EPR spectrum and of the related properties of these materials.

The EPR signals detected before and after X-ray irradiation are separately discussed below, giving them, at least in the second case, specific attribution to a defect structural model. The presence of the identified EPR defects and the effects on their concentration of the steam pressure treatment are then discussed in terms of the possible physical and chemical mechanisms involved in the sample production and hydrothermal ageing of the sintered material.

### 4.1. Spectrum of unirradiated samples

Unirradiated samples give rise to a spectrum dominated by signal (a) at low fields which results from $Fe^{3+}$ impurities, and by the weak and very stable signals (b) and (c) in the region around $g = 2$. The value $g = 2$ and a lack of particular structures do not allow the formulation any hypothesis about the origin of signal (b). Uncertainty also exists about the origin of signal (c): the change in its shape with temperature suggests it might be a superposition of two different signals of which one is subjected to a broadening with increasing temperature. Because saturation is absent, such a signal may be affected by fast processes of spin-lattice relaxation. On the other hand, the observation of the presence of these signals even after a prolonged heating at 850 °C (the temperature at which the mobility of oxygen atoms becomes relevant within this material [1]) allows one to think it very improbable that their origin could be lattice defects involving oxygen vacancies. Moreover, the analysis of the intensities of this kind of signal as a function of the surface/volume ratio, suggests attribution to defects originating on the surface. In fact, measurements on progressively smaller samples obtained by consecutive breaking of the original samples, show no dependence on the volume but rather on the proportion of the original sample surface. The variation of the intensity of one of the components of signal (c) with the treatment in the autoclave also suggests its localization on the surface.

### 4.2. Spectrum of irradiated samples

#### *4.2.1. Signal (A)*

The shape of signal (A) is symmetrical and structured in components with different intensities. This may be a feature of a multiple hyperfine structure (hfs) due to interactions with more than one nuclear spin. In particular, the observed relative intensities (with a maximum for the central signal) is typical of structures due to a hyperfine interaction with identical nuclei at equal distance [14]. In the case of zirconia–yttria material, the nuclei with a spin different from zero that can be present in significative amounts are those of $^{89}Y$ ($I = 1/2$, 100 % natural abundance) and of $^{91}Zr$ ($I = 5/2$, 11 % natural abundance). However, signals of paramagnetic centres interacting with zirconium nuclei should be constituted by a single signal, due to the interaction with the nuclei of the main isotope $^{92}Zr$ ($I = 0$, 89 % natural abundance) overlapping a weak hfs from the interaction with nuclei of $^{91}Zr$ consisting of sextets ($2I + 1 = 6$). The shape of signal (A), however, implies an equivalent interaction with four nuclei of $^{89}Y$, giving rise to five elements with relative intensities 1:4:6:4:1 (see the draft in Fig. 3). A comparison by numerical computation, performed starting from this hypothesis, yields the following parameters: $g = 1.899$, hyperfine splitting of the components $\alpha = 4$ mT, linewidth of the single component 4.5 mT, with gaussian shape of the line.

The origin of this kind of signal could be a $F^+$ centre due to an electron trapped within an oxygen vacancy of a cationic tetrahedron of ions $Y^{3+}$. Values of $g$ of the order of 1.90 were actually observed for $F^+$ centres on other compounds [15]. Because an anionic vacancy surrounded by four trivalent cations could not give rise to an electronic trap in the stabilized

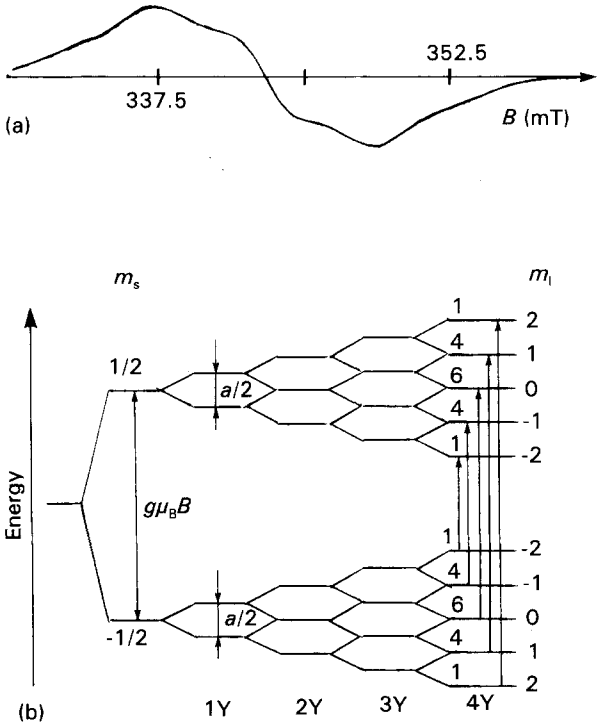


*Figure 3* (a) Computed simulation of signal A and (b) energy-level diagram of the hyperfine interactions with four yttrium nuclei (see text).

zirconia lattice for obvious reasons of charge defect, whereas it could be in the yttrium oxide, the hypothesis formulated implies the presence of $Y_2O_3$ micro-aggregates within the analysed samples. In fact, the oxygen ions are coordinated with four cations in tetrahedral symmetry in the yttrium trioxide, in an approximately regular arrangement [16]. The anionic vacancy is then equidistant at 0.230 nm [17] from the four cations of the first shell; this highly symmetrical coordination justifies the symmetrical shape of the signal. This attribution is also supported by the fact that the amount of experimental hyperfine splitting $\alpha = 4$ mT is in agreement with a theoretically computed estimate on the hypothesis of an $F^+$ centre [15, 18]: assuming the hfs is mainly due to a contact interaction, the computed constant for the hfs interaction matches the experimental one within a factor of 2, even though constrained by the limits imposed by a point charge approximation (see Appendix).

### 4.2.2. Signal (B)

In order to analyse signal (B) induced by the irradiation procedure, all other spectral components must be subtracted from the experimental spectrum. The result of this operation is shown in Fig. 4 in which an asymmetric signal having the typical shape of a powder signal, is seen. A numerical reproduction of the signal obtained with a randomly angular distribution of axial EPR centres gives $g_{||} = 1.85$, $g_\perp = 1.96$, linewidth $\Delta B_{||} = \Delta B_\perp = 3$ mT, and a gaussian distribution of the $g_{||}$ value, corresponding to an inhomogeneous broadening of about 2 mT.

The principal values of the $g$ tensor and the asymmetric shape of the signal suggests that signal (B) is due to a cationic defect (electron trapped in 4d orbitals of $Zr^{4+}$ or $Y^{3+}$) rather than due to an anionic defect (electronic hole in anionic orbitals) or to an $F^+$-like defect. An analysis of the energy levels in the crystalline field was carried out on different possible configurations of cationic defects. The condition $g_{||} \leq g_\perp$ for ions $4d^1$ (pertaining to $Zr^{3+}$ and $Y^{2+}$) is satisfied only in eight-fold (cubic) and four-fold (tetrahedral) coordinations with tetragonal distortion (elongation of the $c$-axis). The following remarks may also be made.

1. The eight-fold coordination must be ruled out because the cationic sites thus coordinated have no defects of negative charge and consequently they cannot be electronic traps able to capture electrons in 4d orbitals.

2. The four-fold coordination must also be ruled out in the stabilized zirconia structure, because it requires the contemporary presence of four oxygen vacancies for each defect site: a very improbable condition to take place.

3. The four-fold coordination could, instead, have a high probability to occur in the structure of the yttria where only two oxygen vacancies are involved with respect to the normal six-fold coordination of yttrium ions.

Thus, signal (B) seems to provide further evidence of the existence of a cluster of nuclei of $Y_2O_3$ inside the structure of the Y-TZP samples. Inhomogeneous broadening of the EPR signal may be related to a statistical structural disorder originating from a tetragonal distortion differing slightly from one defect site to another. By the adoption of the unit cell parameters of $Y_2O_3$, the $\langle r^2 \rangle$ and $\langle r^4 \rangle$ and $\lambda$ values of the 4d orbital of the $Y^{2+}$ ion [19], the elongation of the $c$-axis is found to vary over a reasonable range between 0.0005 and 0.0015 nm.

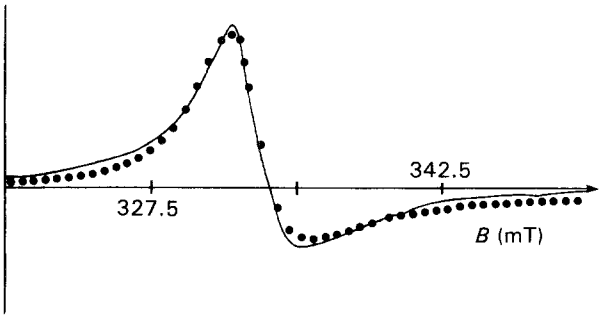


*Figure 4* EPR spectrum of signal B, obtained after subtraction of the other overlapping signals (——), and (●) computed simulation (see text).

## 4.3. Effects of autoclave treatment

The EPR spectrum of the irradiated samples submitted to treatment in an autoclave does not substantially differ from that of the untreated samples, except in the lower intensity of signal (A).

The treatment has in some way decreased the efficiency of the creation of EPR centres by irradiation, with a modification of the surface structure of the material. A diffusion process of some ionic species could have taken place, connected with the steam present under pressure in the autoclave. The consequent atomic structural rearrangement may have played a compensating role in the process of the creation of the defects. Such phenomena have been observed in other materials such as silicon dioxide [20] in which the hydrogen assumes a radioprotective function.

## 5. Conclusions

The identification of the EPR defects observed in sintered Y-TZP allows certain aspects of the structure of this material to be considered.

1. The X-ray-induced EPR signals (A) and (B) indicate the presence of $Y_2O_3$ aggregates in all the analysed samples. Both types of defect involve the presence of oxygen vacancies in lattice sites such as an $F^+$ centre (signal A) or $Y^{2+}$ ion (signal B).

2. The absence in X-ray irradiated samples of the EPR signal attributed to six-fold coordinated $Zr^{3+}$ ions [11] in observed single crystals of stabilized zirconia, containing about the same nominal concentration of $Y^{3+}$, suggests that the concentration of oxygen vacancies in the zirconia lattice in the surface region affected by irradiation is lower than that expected, probably because of the presence of $Y_2O_3$ aggregates.

The autoclave treatment does not produce strong modification of the EPR spectra; nor are new signals observed. Nevertheless, some remarks may be made about the lower intensity of the EPR signal (A) and the higher intensity of the signal (c) after the autoclave treatments.

3. Because signal (A) has been attributed to $F^+$-like centres constituted by oxygen vacancies coordinated to four $Y^{3+}$ ions, its lower intensity may be related to the treatment-induced modification of the $F^{2+}$ diamagnetic precursor defect site in a radiation-resistant form. This agrees with the formation of $Y(OH)_3$ clusters as observed by Lange *et al.* [7].

4. The increase in the intensity of signal (c) observed in all the samples may be interpreted as a modification of the surface structure. Because its thermal stability and spectroscopic features rule out that it arises from oxygen vacancies, it may be an indication of an increase in structural phases different from the tetragonal or cubic ones (e.g. the monoclinic phase). The corresponding X-ray diffractometric spectra always show a predominance of tetragonal phase, but with the appearance of a small amount of monoclinic phase after autoclave treatment.

In reality, the observed changes of the EPR spectra are found to be sensitive to the consequent modifications of the material, because they pertain to relatively short hydrothermal treatments.

## Acknowledgements

This work was carried out within the "Progetto Finalizzato Materiali speciali per Tecnologie Avanzate" research program of the Italian National Research Council (CNR). The authors are particularly indebted to Idema Venturi, technician at IRTEC-CNR, for her cooperation given in carrying out the autoclave treatment of the samples and to Sante Monteforte, student, Instituto Superiore per le Industrie Artistiche (ISIA) of Faenza, for his efficient help with the experimental preparations. F. Meschke is a bursary holder of the EEC Brite-Euram programme.

## Appendix

By assuming the hfs is mainly due to a contact interaction (as it generally is for F centres for which the hf anisotropic interaction is much lower than the isotropic one [15]), the constant for the hf interaction is given by [18]

$$a = \tfrac{8}{3}\pi g_e \mu_B g_N \mu_N A_R |\phi_F(R)|^2 \qquad (A1)$$

where $\mu_B$ and $\mu_N$ are the Bohr and nuclear magnetons, $g_e$ and $g_N$ the electron and nuclear $g$ values, and $\phi_F(R)$ the envelope function of the $F^+$ centre for which the wave function can be expressed by the electronic wave functions, $\psi_i$, of the ions of the first shell

$$\psi_F = N(\phi_F - \sum_i \psi_i \langle \psi_i | \phi_F \rangle) \qquad (A2)$$

where $N$ is a normalization factor. In Equation A1, is a factor relating the mean electronic density $|\psi_F|^2$ of the nucleus with the value $|\phi_F|^2$ given by only that part of the envelope of the wave function of the $F^+$ centre, which is roughly proportional to $R^3$. Thus

$$a = \tfrac{8}{3}\pi g_e \mu_B g_N \mu_N A_R k/R^3 \qquad (3)$$

where $k$ is a constant and $A_R$ is a simple function of $Z^{3/2}$ in a first approximation, where $Z$ is the atomic number of the first-shell ions. The value of $k$ is empirically found, by experimental collections of $\alpha$, to be around $12.7 \times 10^{-3} \pm 4.5 \times 10^{-3}$.

## References

1. E. C. SUBBARAO and H. S. MAITI, *Solid State Ionics* **11** (1984) 317.
2. K. KOBAYASHI, H. KUWAJIAMA and T. MASAKI *ibid.* **3** (1981) 489.
3. J. J. SWAB, *J. Mater. Sci.* **26** (1991) 6706.
4. T. SATO and M. SHIMADA, *J. Am. Ceram. Soc.* **68** (1985) 356.
5. M. YOSHIMURA, T. NOMA, K. KAWABATA and S. SOMIYA, *J. Mater. Sci. Lett.* **6** (1987) 465.
6. M. YOSHIMURA, T. NOMA, K. KAWABATA and S. SOMIYA, *J. Ceram. Soc. Jpn. Int. Ed.* **96** (1988) 263.
7. F. F. LANGE, G. L. DUNLOP and B. I. DAVIS, *J. Am. Ceram. Soc.* **69** (1986) 237.
8. A. J. A. WINNBST and A. J. BURGGARAAF, in "Advances in Ceramics, Science and Technology of Zirconia III", edited by S. SOMIYA, N. YAMAMOTO and H. HANAGIDA, (American Ceramic Soc. Columbus, OH, 1988) p. 39.
9. C. B. AZZONI and A. PALEARI, *Solid State Ionics* **44** (1991) 267.
10. V. M. ORERA, R. I. MERINO, Y. CHEN, R. CASES and P. J. ALONSO, *Phys. Rev. B* **42** (1990) 9782.
11. C. B. AZZONI and A. PALEARI, *ibid.* **44** (1991) 6858.
12. S. MONTEFORTE, ISIA Thesis, Faenza (1992).
13. D. L. GRISCOM, *J. Non-Cryst. Solids* **40** (1980) 211.
14. J. E. WERTZ and J. R. BOLTON, "Electron Spin Resonance" (Chapman and Hall, New York, 1986).
15. H. SEIDEL and H. C. WOLF, in "Physics of Color Centers", edited by W. B. FOWLER (Academic Press, New York 1968) p. 538.
16. A. F. WELLS,"Structural Inorganic Chemistry" (Clarendon Press, Oxford, 1975).
17. R. W. G. WYCKOFF, "Crystal Structure", (Wiley, New York, 1963).
18. A. E. HUGHES and B. HENDERSON, in "Point Defects in Solids", Vol I, edited by J. H. CRAWFORD Jr and L. M. SLIFKIN, (Plenum Press, New York, 1972) p. 381.
19. A. ABRAGAM and B. BLEANEY, "Electron Paramagnetic Resonance of Transition Ions", (Clarendon Press, Oxford, 1970) p. 474.
20. R. A. B. DEVINE, *J. Non-Cryst. Solids* **107** (1988) 41.

*Received 7 August 1992*
*and accepted 4 January 1993*